coatings

MDPI

Article

Damping Properties of Arc Ion Plating NiCrAlY Coating with Vacuum Annealing

Guangyu Du [1,*], Zhen Tan [1,2], Guohao Li [1], Dechun Ba [1] and Kun Liu [1]

[1] Key Laboratory of Vibration and Control of Aeronautical Equipment, Ministry of Education, Northeastern University, Shenyang 110819, China; tanz_hen@126.com (Z.T.); liguohao369@163.com (G.L.); dchba@mail.neu.edu.cn (D.B.); kliu@me.neu.edu.cn (K.L.)

[2] Institute of Technology, Shenyang Radio and TV University, Shenyang 110004, China

* Correspondence: gydu@mail.neu.edu.cn; Tel.: +86-24-8367-6945

Received: 5 December 2017; Accepted: 28 December 2017; Published: 3 January 2018

Abstract: NiCrAlY coating was prepared on a stainless steel substrate by an arc ion plating machine and the annealing experiments were carried out at different temperatures using a tube furnace. The effects of annealing temperatures on the morphology, structure, chemical composition and phase structure of the coating were characterized by SEM, EDS and XRD, respectively. The change of microstructure is discussed. Dynamic mechanical analyzer results determined the suitable annealing temperature for the best damping performance. The effect of annealing temperature on the microstructure and damping properties of NiCrAlY coating are also discussed. The relationship between annealing temperature and damping properties are explained by microstrcuture, grain size and phase structure.

Keywords: damping property; NiCrAlY; annealing; microstructure

1. Introduction

As the modern aeroengine gradually develops to be resistant to high temperature, high pressure and high rotating speeds, the problem of fatigue breakdown of key components caused by overvibration has become prominent. It has been confirmed that one main reason for the failure within an aircraft engine is high cycle fatigue [1,2]. Therefore, it is urgent to suppress the vibration effectively and reduce the damage resulting from it. There are three common methods to solve the problem of vibration, which are system damping, material damping and structural damping [3] System damping is to install a damping shock absorber in the system, but this is not suitable for the harsh environment. Structural damping is to apply coating to the affected parts to prepare a reliable composite structure. Due to its advantages of light weight and a simple structure, the traditional viscoelastic polymer coating is used widely [4]. However, the low working temperature and the vulnerability limit its further application. Therefore, research into the damping properties of hard coatings has gradually aroused the interest of researchers [5]. Representative hard coatings include NiCrAlY coating and other ceramic coatings [6–8]. NiCrAlY coating is the main component of thermal barrier coating; its anti-oxidation properties at high temperature have been widely studied and applied [9–11]. However, some researchers found that NiCrAlY coatings also have excellent damping properties in addition to their thermal insulation properties. Yu [12] prepared NiCrAlY coatings by plasma spraying and the damping properties of the coating have been discussed. The damping mechanism of the interaction between the substrate and the coating has also been proposed. Obrtlík [13] studied the low cycle fatigue behavior of thermal barrier coatings at 900 °C, and discussed the difference between the fatigue behavior of the coating and that of the uncoated substrate.

The working environment of aircraft engine blades is very harsh [14,15]. As a key part of thermal barrier coating, the study of the mechanical properties of the NiCrAlY coating is very important.

Some researchers have reported much work on this [16–18]. Ghidelli [19,20] studied the measurement method of residual stress and fracture mechanics of the coating. Although the NiCrAlY coating has been extensively studied by many researchers, the research on the damping properties of NiCrAlY coating is still not sufficient, and more research is required. There are a few reports about the effect of processing parameters such as vacuum annealing on the damping properties of NiCrAlY coating. Vacuum annealing can not only refine the grain and change the microstructure of the coating, but also lessen the microscopic defects of the coating.

In this paper, the NiCrAlY coating was prepared on the substrate by arc ion plating, and the coating samples were annealed under different annealing temperatures. The microstructure, phase structure and chemical composition of the coating samples were characterized by scanning electron microscopy and X-ray diffraction. Moreover, the damping properties of the coatings were measured by dynamic mechanical analyzer. The test results offer a basis for the analysis of the effect of annealing temperature on the microstructure and damping properties of NiCrAlY coating.

2. Materials and Methods

The NiCrAlY coating was deposited on stainless steel substrates (60 mm × 10 mm × 0.5 mm) by arc ion plating (FMA90/80 Top-Eastern Vacuum TECH. Co. LTC., Dalian, China). The target was 60Ni-33.7Cr-4.5Al-1.8Y (wt %) alloy. The stainless steel substrate obtained by wire cutting was fully pre-treated before the preparation. The surface of the substrate was polished with sandpaper to remove the surface oxides, and the substrate surface was processed by polishing instrument. Before being loaded into the equipment, the substrate was cleaned by ultrasonic in acetone solution. Pretreatment can increase the adhesion of the coating to the substrate and the corresponding mechanical properties of the coating [21,22].

Before the Ar gas (99.99% pure) entranced, a pressure of 1×10^{-3} Pa was obtained in the sputtering chamber by a turbo molecular pump. The working pressure was 1 Pa and the distance between the substrates and the target was 100 mm. The arc current was 60 A and the substrate bias was 200 V. The deposition time was 2 h and the deposition thickness was 15 μm. After deposition, the samples were annealed at 873, 973, 1073, 1173 and 1273 K for 2 h at the pressure of 3×10^{-3} Pa (Figure 1). The annealing experiment employed a JKQF-13000 tube annealing furnace (Jinan Precision Scientific Instrument and Meter Co. Ltd., Jinan, China).

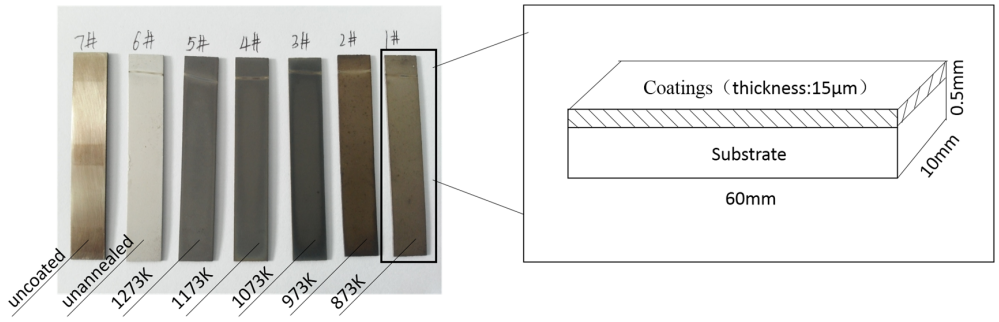

Figure 1. Test samples after vacuum annealing.

The elemental composition was determined through energy dispersive spectrograph analysis (SSX-550 Shimadzu, Kyoto, Japan). The microstructure of the coating was observed by X-ray diffraction (PW3040/60 PANalytical B.V, Almelo, Holland)with Cu Kα1 radiation (λ = 1.5406 Å) and a 2θ angle was in the range of 5°–90° with a step size of 0.033°.The surface morphology of the coatings was observed by scanning electron microscope (SSX-550 Shimadzu, Kyoto, Japan). The CSM hardness scratch tester (CSM Instruments SA, Buchs, Switzerland) was used to test the bonding force between the coating and the substrate.

In order to characterize the basic damping properties of coating samples, proper methods must be considered. The damping properties of hard coating were usually characterized as damping capacity (Q^{-1}). The Q^{-1} was tested by dynamic mechanical analyzer (DMA) according to the three-point bending method. The test temperature was 30 °C.

The dissipation of the external energy is the embodiment of the damping property of the coating.

According to the definition of complex modulus [23]:

$$E^* = \frac{\sigma}{\varepsilon} = \frac{\sigma_0}{\varepsilon_0} e^{i\alpha} = E(\cos\varphi + \sin\varphi) \quad (1)$$

$$E^* = E' + iE'' = E'\left(1 + iQ^{-1}\right) \quad (2)$$

Q^{-1} is the damping coefficient (known as the loss factor) of the coating, which can be expressed as the ratio of dissipated energy and stored energy in each cycle of vibration. The relationship can be expressed as:

$$Q^{-1} = \frac{E'}{E''} = \tan\varphi \quad (3)$$

E^* is the complex modulus, E' is the real parts of the complex modulus, called storage modulus.

$$E' = E\cos\varphi \quad (4)$$

E'' is the imaginary parts of the complex modulus, called loss modulus.

$$E'' = E\sin\varphi = Q^{-1}E' \quad (5)$$

In which E'' and E' are loss modulus and storage modulus.

Loss factor Q^{-1} is commonly used to characterize the damping properties of the coatings. The increasing of loss factor Q^{-1} means the better damping performance of the coating.

3. Results

3.1. Analysis of Binding Force and Hardness

A CSM hardness scratch tester was used to test the bonding force between the coating and the substrate. The load range of the test instrument was 50–500 mN. Since the binding force of the NiCrAlY coating and the stainless steel substrate is relatively large, there was no coating falling off or delamination phenomenon on the surface of the coating when the scratch tester was loaded to 500 mN. Therefore, the adhesion force between the NiCrAlY coating and the stainless steel substrate was higher than 500 mN, and the combination was ideal. The morphology of the NiCrAlY coating specimen under the CSM scratch tester is shown in Figure 2. The binding force between the coating and the substrate of the samples prepared at different annealing temperatures is similar, and the value of the coating is more than 500 mN.

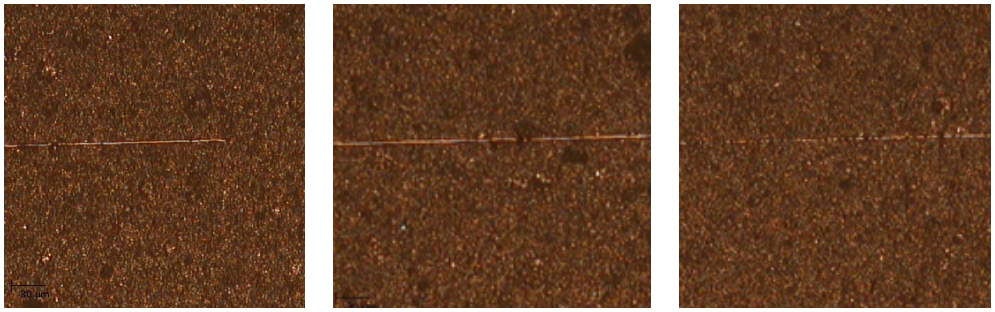

Figure 2. Morphology of NiCrAlY coating sample after the scratch tester testing.

The hardness of the coating was tested by the CSM hardness scratch tester. Figure 3 shows the surface hardness of the samples at different annealing temperatures. There is no definite rule for the hardness of the coating with the change of annealing temperature. The hardness of the material is closely related to the atomic arrangement of the constituent materials, the number of grain boundaries, the types of elements, and the thermal treatment process. The change of the vickers hardness value (HV) of the NiCrAlY coating may be related to the Cr content of the coating. The surface hardness is the largest when the highest Cr content is 1273 K.

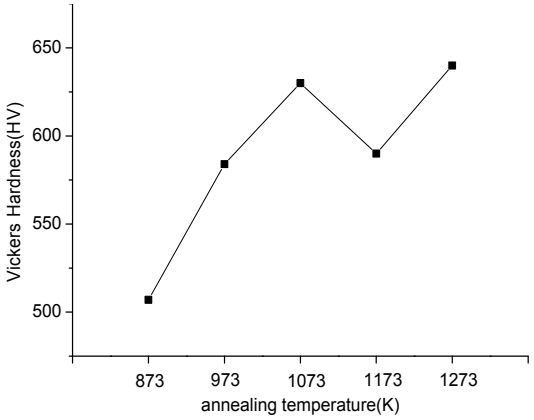

Figure 3. Vickers hardness of NiCrAlY coating.

3.2. Structural Study

The phase structure of the NiCrAlY coating will change obviously after the vacuum heat treatment. In order to study the change, the surface of the coating was analyzed by XRD. The results are shown in Figure 4.

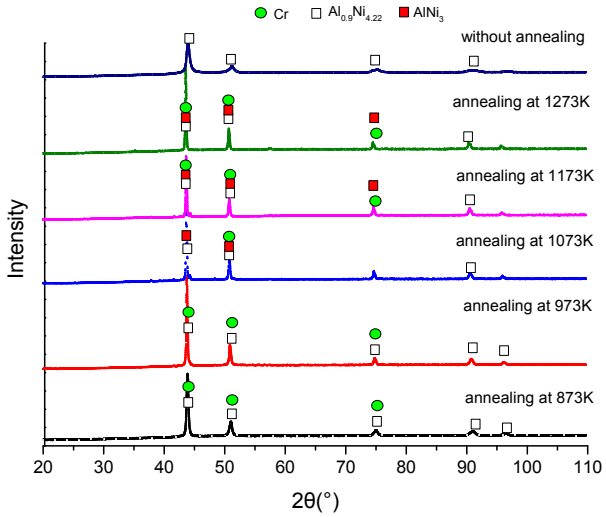

Figure 4. XRD diagram of NiCrAlY coating prepared at different vacuum annealing temperatures.

The deposited NiCrAlY coating without vacuum annealing consists of γ-Ni, β-NiAl, and α-Cr phases. The diffraction peaks are sharp and high. The phase structure of the NiCrAlY coatings are unchanged after vacuum annealing at 873 K and 973 K. The higher intensity of the diffraction peaks confirmed the improvement of the crystallinity of the coating after vacuum annealing. The γ′-Ni3Al phase was precipitated in the coating at 1073 K and 1173 K. According to the isothermal sections of Ni-Cr-Al ternary phase diagram, it is concluded that during the vacuum heat process the reaction:

γ-Ni(Cr) + β-NiAl → γ′-Ni3Al + α-Cr happened. However, the γ zone significantly enlarged when the temperature is elevated further. The increased intensity of the γ′-Ni3Al diffraction peak suggests that the content of γ′-Ni3Al improved significantly.

The grain size can be calculated by the Scherrer formula.

$$D = \frac{K\lambda}{\beta_{hkl} \cos\theta} \quad (6)$$

In which K is the Scherrer constant. K = 0.89, β_{hkl} is the half width of diffraction peak, λ is the X wavelength of XRD used for testing, λ = 0.154059 nm, θ is the diffraction angle, D is the grain diameter. The full width at half maximum (FWHM) of the characteristic peak was selected for the calculation of the grain size.

Table 1 shows the grain size of the coatings at different annealing temperatures. Compared with the unannealed coating, the grain size of the NiCrAlY coating is obviously increased by annealing. With the increase of annealing temperature, the particles of the coating particles turn to be obviously agglomerated. The size of the grain will become larger when the grain is regrown.

Table 1. Grain size of the NiCrAlY coating calculated by Scherrer.

Annealing Temperature	β_{hkl}	Diffraction Angle (θ)	Grain Size (nm)
873 K	0.292248	43.97749	0.65197
973 K	0.227304	43.84206	0.836341
1073 K	0.194832	43.76009	0.974395
1173 K	0.227304	43.73519	0.83485
1273 K	0.194832	43.66181	0.972643
Unannealing	0.32472	44.00944	0.587164

3.3. Surface Morphological And Compositional

Figure 5 shows the surface microstructures of NiCrAlY coating at different vacuum annealing temperatures.

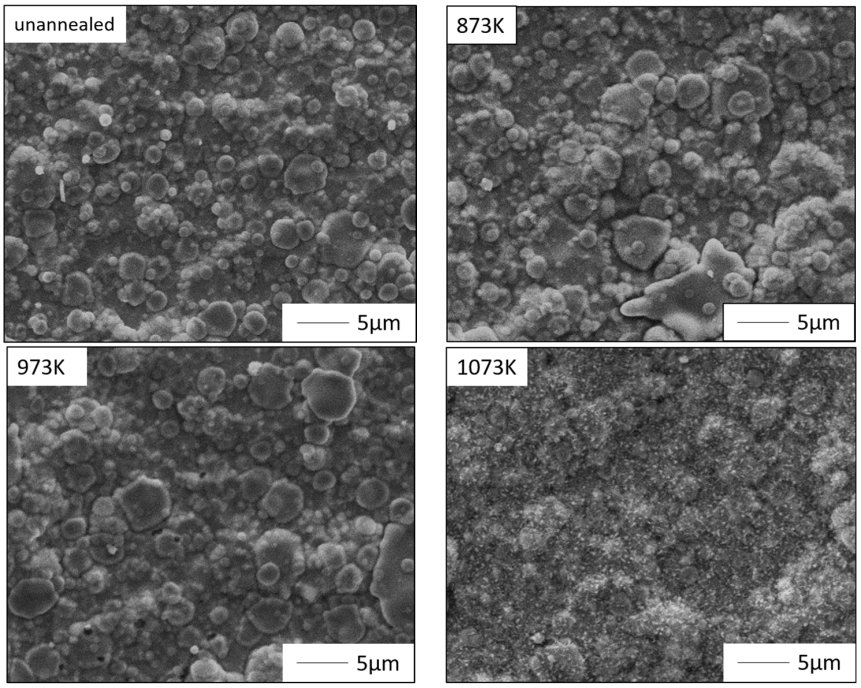

Figure 5. *Cont.*

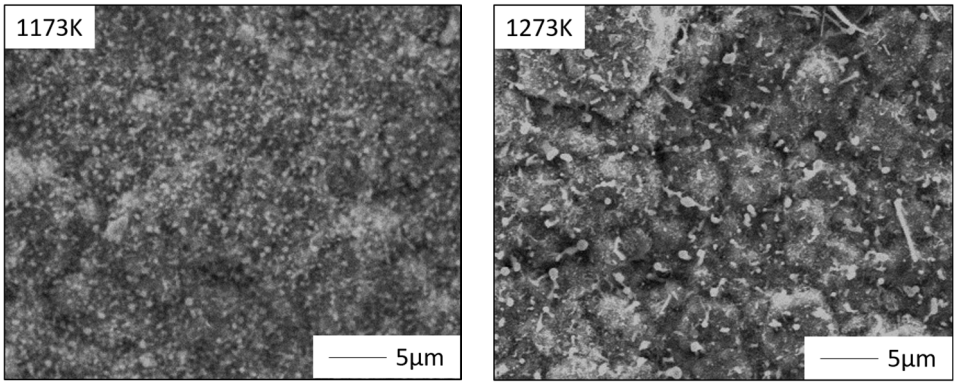

Figure 5. Surface morphology of NiCrAlY coating prepared at different vacuum annealing.

It was observed that the coating without vacuum annealing was composed of metal drops. The surface of the coating is granular, and the surface particles show an obviously agglomerated trend. Many unevenly sized pellets cause the rough surface. At the annealing temperature of 873 K and 973 K, the particles have a tendency to mutual fusion. Metal drops fused together. The melting of different particles inside the coating causes the release of internal stress between particles, which make many micro-cracks and voids on the surface of the coating. Micro-cracks and large pores appear on the surface. When the annealing temperature is at 1073 K, the surface of the coating melts obviously, and the surface of the coating becomes flat. Defects in the coating can be filled. When the annealing temperature is over 1073 K, there are no obvious boundaries between the coating particles, which means that the particles of the coating surface are interfused at a high annealing temperature.

The chemical composition of the coating was measured by EDS (Figure 6). The process of vacuum annealing will cause the diffusion of elements. At 873 and 973 K, The average weight percent (wt %) of Ni, Cr and Al in coating has no obvious change compared to that in the coating without vacuum annealing. When the annealing temperature is over 1073 K, the Cr element in the coating diffuses to the substrates, and the Al element diffuses from the substrates to the coating, which results in the increase of Cr and the decrease of Al. According to the results of the EDS analysis, at different annealing temperatures, the elements in the coating diffuse, which causes an irregular change in the surface elements of the coating. As for the results of XRD, the production of a new crystal structure leads to large changes in the surface elements of the coating.

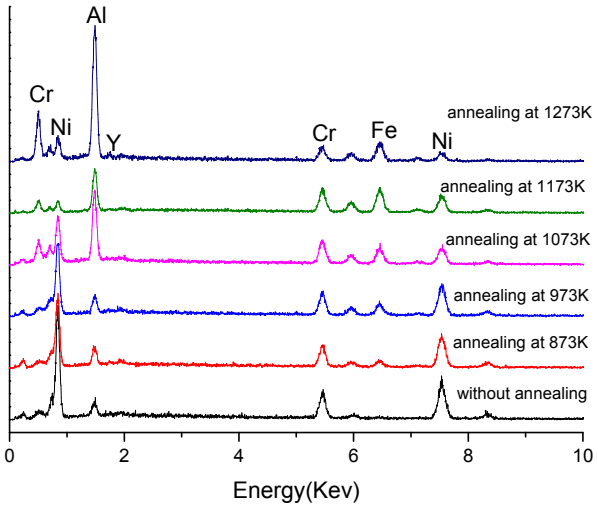

Figure 6. Energy spectrum of NiCrAlY coating prepared at different vacuum annealing temperatures.

3.4. Damping Properties

In the frequency-scanning test of the loss factor of the NiCrAlY coating, the operating temperature was 30 °C, the strain was 0.05% and the frequency range was 115–180 Hz. Figure 7 shows the result.

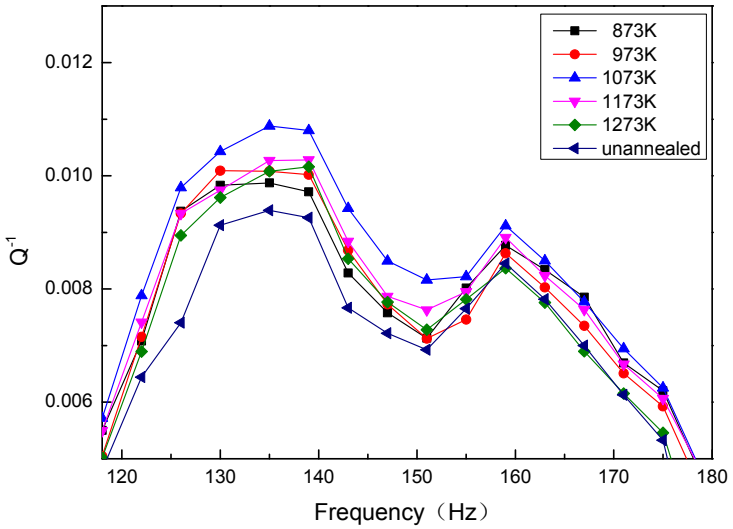

Figure 7. Damping capacity with different vacuum annealing temperatures at 0.05% strain.

In the process of increasing frequency, damping values of samples show a nonlinear fluctuation between 0.005 and 0.011, which relate to the natural frequency of the substrate material.

4. Discussion

The result of the CSM show the binding force between coating and substrate over 500 mN under the different annealing temperatures, which proves a good combination between the coating and substrate. By analyzing the XRD results, Ni3Al appeared at 1073 K. It is reported that the Ni3Al structure has a reticulum which can lead to energy consumption by internal friction when external motivation acts on the coating [24]. It can be seen from Figure 4 that the content of Ni3Al gradually increases with the increase of annealing temperature. In theory, this is beneficial to the damping properties. However, the coating at the annealing temperature of 1073 K showed the best damping performance under the vibration frequency from 115 to 180 Hz. Therefore, there are still other microstructures which have a significant effect on the damping performance.

According to Figure 5, the surface of the NiCrAlY coating possesses both a large melt drop structure and suitable crystalline particles refined by annealing at the annealing temperature 1073 K. In the condition of low annealing temperature or no annealing, the melt state is filled with microscopic defects such as micro-voids and micro-cracks in the process of the formation of large surface-melting particles. There are no advantages to improving the damping performance of the coatings. The enhancement of the annealing temperature can lead to the increase of grain size and the refinement of the coating surface obviously, this is proved by the surface morphology of the coatings annealed at 1173 K and 1273 K in Figure 5. Research has shown that the increase in grain size is not conducive to the improvement of the coating damping performance [25].

Therefore, the coating constituted by the reticulum, suitable grain size and sufficient microscopic defects shows the best damping performance at the annealing temperature of 1073 K. This kind of structure can improve the damping performance of the coating through the interface slip and grain boundary friction energy dissipation under the condition of excitation.

5. Conclusions

In this paper, the effect of vacuum annealing on the damping properties of an NiCrAlY coating was investigated. The NiCrAlY coating prepared by arc ion plating had good bonding force. The damping value of the sample shows a nonlinear fluctuation with the increasing temperature. The best damping performance was exhibited at 1073 K in this paper. The reduction of small particles and defect structures was caused by the increased annealing temperature. When the annealing temperature is 1073 K, the coating forms an Ni3Al phase, which has a reticulum structure.

When the annealing temperature is 1073 K, under the action of external load, the defect structure and Ni3Al reticulum structure of the coating can achieve the dissipation of the external load, which is conducive to the improvement of the damping properties of the coating.

Acknowledgments: This work was financially supported by Funds for Basic Scientific Research Funds for Central Universities (N160304002, N160302001, N140301001), Key Laboratory of Vibration and Control of Aeronautical Equipment, Ministry of Education, Northeastern University (VCAME201604), National Natural Science Foundation of China (51005043).

Author Contributions: Guangyu Du and Zhen Tan conceived and designed the experiment; Dechun Ba searched literature; Guohao Li performed the experiment and collected data; Guangyu Du, Zhen Tan, Kun Liu, Dechun Ba analyzed the data and designed the figures and table; Guangyu Du, Guohao Li wrote the paper.

Conflicts of Interest: The authors declare no conflict of interest.

References

1. Al-Anazi, D.; Hashmi, M.S.J.; Yilbas, B.S. High-velocity oxy-fuel thermally sprayed CoNiCrAlY coatings on Ti-6Al-4V alloy: High cycle fatigue properties of coating. *Proc. Inst. Mech. Eng. Part B J. Eng. Manuf.* **2007**, *221*, 647–654. [CrossRef]
2. Musalek, R.; Kovarik, O.; Medricky, J.; Curry, N.; Bjorklund, S.; Nylen, P. Fatigue testing of TBC on structural steel by cyclic bending. *J. Therm. Spray. Technol.* **2014**, *24*, 168–174. [CrossRef]
3. Lakes, R.S. High Damping Composite Materials: Effect of Structural Hierarchy. *J. Compos. Mater.* **2002**, *36*, 287–297. [CrossRef]
4. Treviso, A.; van Genechten, B.; Mundo, D.; Tournour, M. Damping in composite materials: Properties and models. *Compos. Part B Eng.* **2015**, *78*, 144–152. [CrossRef]
5. Blackwe, C.; Palazotto, A.; George, T.J.; Cross, C.J. The evaluation of the damping characteristics of a hard coating on titanium. *Shock. Vib.* **2007**, *14*, 37–51. [CrossRef]
6. Levi, C.G.; Sommer, E.; Terry, S.G.; Catanoiu, A.; Rühle, M. Alumina grown during deposition of thermal barrier coatings on NiCrAlY. *J. Am. Ceram. Soc.* **2002**, *86*, 676–685. [CrossRef]
7. Niki, T.; Ogawa, K.; Shoji, T. Mechanical and High Temperature Oxidation Properties of Cold Sprayed CoNiCrAlY Coating for Thermal Barrier Coating. *J. Solid Mech. Mater. Eng.* **2008**, *2*, 739–747. [CrossRef]
8. Liu, Z.H.; Yang, H.B.; Jia, Y.F.; Shu, X. Heat protective properties of NiCrAlY/Al_2O_3, gradient ceramic coating fabricated by plasma spraying and slurry spraying. *Surf. Coat. Technol.* **2017**, *327*, 1–8. [CrossRef]
9. Chen, W.R.; Wu, X.; Marple, B.R.; Patnaik, P.C. Oxidation and crack nucleation/growth in an air-plasma-sprayed thermal barrier coating with NiCrAlY bond coat. *Surf. Coat. Technol.* **2005**, *197*, 109–115. [CrossRef]
10. Patterson, T.; Leon, A.; Jayaraj, B.; Liu, J.; Sohn, Y.H. Thermal cyclic lifetime and oxidation behavior of air plasma sprayed CoNiCrAlY bond coats for thermal barrier coatings. *Surf. Coat. Technol.* **2008**, *203*, 437–441. [CrossRef]
11. Waki, H.; Kobayashi, A. Influence of the mechanical properties of CoNiCrAlY under-coating on the high temperature fatigue life of YSZ thermal-barrier-coating system. *Vacuum* **2008**, *83*, 171–174. [CrossRef]
12. Yu, L.M.; Ma, Y.; Zhou, C.G.; Xu, H.B. The Influence of NiCrAlY Coatings Prepared by LPPS and EB-PVD on the Damping Properties of 1Cr18Ni9Ti Alloy. *Mater. Sci. Forum.* **2005**, *475–479*, 3971–3976. [CrossRef]
13. Obrtlík, K.; Hutařová, S.; Čelko, L.; Juliš, M.; Podrábský, T.; Šulák, I. Effect of Thermal Barrier Coating on Low Cycle Fatigue Behavior of Cast Inconel 713LC at 900 °C. *Adv. Mater. Res.* **2014**, *891–892*, 848–853. [CrossRef]

14. Calleja, A.; Fernández, A.; Rodríguez, A.; de Lacalle, L.N.L.; Lamikiz, A. Turn-milling of blades in turningcentres and multitasking machines controlling tool tilt angle. *Proc. Inst. Mech. Eng. Part B J. Eng. Manuf.* **2014**, *229*, 1324–1336. [CrossRef]
15. Beranoagirre, A.; de Lacalle, L.N.L. Turning of gamma TiAl intermetallic alloys. *Procedia Eng.* **2013**, *63*, 489–498. [CrossRef]
16. Li, W.Z.; Wang, Q.M.; Bao, Z.B.; Yao, Y.; Gong, J.; Sun, C.; Jiang, X. Microstructural evolution of the NiCrAlY/CrON duplex coating system and its influence on the mechanical properties. *Mater. Sci. Eng. A* **2008**, *498*, 487–494. [CrossRef]
17. Waki, H.; Kitamura, T.; Kobayashi, A. Effect of Thermal Treatment on High-Temperature Mechanical Properties Enhancement in LPPS, HVOF, and APS CoNiCrAlY Coatings. *J. Therm. Spray Technol.* **2009**, *18*, 500–509. [CrossRef]
18. Torvik, P.J. Determination of mechanical properties of non-linear coatings from measurements with coated beams. *Int. J. Solids Struct.* **2009**, *46*, 1066–1077. [CrossRef]
19. Ghidelli, M.; Sebastiani, M.; Collet, C.; Raphael, G. Determination of the elastic moduli and residual stresses of freestanding Au-TiW bilayer thin films by nanoindentation. *Mater. Des.* **2016**, *106*, 436–445. [CrossRef]
20. Ghidelli, M.; Sebastiani, M.; Johanns, K.E.; Pharr, G.M. Effects of indenter angle on micro-scale fracture toughness measurement by pillar splitting. *J. Am. Ceram. Soc.* **2017**, *100*, 5731–5738. [CrossRef]
21. Polvorosa, R.; Suárez, A.; de Lacalle, L.N.L.; Cerrillo, I.; Wretland, A.; Veiga, F. Tool wear on nickel alloys with different coolant pressures: Comparison of Alloy 718 and Waspaloy. *J. Manuf. Process.* **2017**, *26*, 44–56. [CrossRef]
22. Rodríguez-Barrero, S.; Fernández-Larrinoa, J.; Azkona, I.; Lópezde Lacalle, L.N.; Polvorosa, R. Enhanced Performance of Nanostructured Coatings for Drilling by Droplet Elimination. *Mater. Manuf. Process.* **2014**, *31*, 593–602. [CrossRef]
23. Yu, L.; Ma, Y.; Zhou, C.; Xu, H. Damping efficiency of the coating structure. *Int. J. Solids Struct.* **2005**, *42*, 3045–3058. [CrossRef]
24. Cui, H.Z.; Wei, N.; Zeng, L.L.; Wang, X.B.; Tang, H.J. Microstructure and formation mechanism of Ni-Al intermetallic compounds fabricated by reaction synthesis. *Trans. Nonferrous Met. Soc. China* **2013**, *23*, 1639–1645. [CrossRef]
25. Sutou, Y.; Omori, T.; Koeda, N.; Kainuma, R.; Ishida, K. Effects of grain size and texture on damping properties of Cu–Al–Mn-based shape memory alloys. *Mater. Sci. Eng. A* **2006**, *438–440*, 743–746. [CrossRef]